Name of Journal; HYDROLOGICAL PROCESSES
Vol.; 15
Page; 1459-1476
Published; June 2001

Seasonal Variation in the Energy and Water Exchanges above and below a Larch Forest in Eastern Siberia

Takeshi OHTA[1, 7], Tetsuya HIYAMA[2, 7], Hiroki TANAKA[3], Takashi KUWADA[4] , Trofim C. MAXIMOV[5], Tetsuo OHATA[6,7] and Yoshihiro FUKUSHIMA[2,7]

[1] Faculty of Agriculture, Iwate University, Morioka 020-8550, JAPAN
[2] Institute for Hydrospheric-Atmospheric Sciences, Nagoya University, Nagoya 464-8601, JAPAN
[3] Graduate School of Agriculture, Kyoto University, Kyoto 606-8502, JAPAN
[4] Faculty of Agriculture, Okayama University, Okayama 700-8530, JAPAN
[5] Institute for Biological Problems of Cryolithozone, Yakutsk 677891, RUSSIA
[6] Institute of Low Temperature Science, Hokkaido University, Sapporo 060-0819, JAPAN
[7] Frontier Research System for Global Change, Tokyo 105-6791, JAPAN

Correspondence should be addressed to:

Takeshi OHTA
Faculty of Agriculture, Iwate University, Morioka 020-8550, JAPAN
Tel/Fax: +81-19-621-6137
E-mail: takeshi@iwate-u.ac.jp

ABSTRACT

The water and energy exchanges in forests form one of the most important hydro-meteorological systems. There have been far fewer investigations of the water and heat exchange in high latitude forests than of those in warm, humid regions. There have been few observations of this system in Siberia for an entire growing season, including the snowmelt and leaf fall seasons. In this study, the characteristics of the energy and water budgets in an eastern Siberian larch forest were investigated from the snowmelt season to the leaf fall season. The latent heat flux was strongly affected by the transpiration activity of the larch trees and increased quickly as the larch stand began to foliate. The sensible heat dropped at that time, although the net all-wave radiation increased. Consequently, the seasonal variation in the Bowen ratio was clearly "U"-shaped, and the minimum value (1.0) occurred in June and July. The Bowen ratio was very high (10 - 25) in early spring, just before leaf opening. The canopy resistance for a big leaf model far exceeded the aerodynamic resistance and fluctuated over a much wider range. The canopy resistance was strongly restricted by the saturation deficit, and its minimum value was 100 sec m^{-1} (10 mm sec^{-1} in conductance). This minimum canopy resistance is higher than values obtained for forests in warm, humid regions, but is similar to those measured in other boreal conifer forests. It has been suggested that the senescence of leaves also affects the canopy resistance, which was higher in the leaf fall season than in the foliated season. The mean evapotranspiration rate from 21 April 1998 to 7 September 1998 was 1.16 mm day^{-1}, and the maximum rate, 2.9 mm day^{-1}, occurred at the beginning of July. For the growing season from 1 June - 31 August, this rate was 1.5 mm day^{-1}. The total evapotranspiration from the forest (151 mm) exceeded the amount of precipitation (106 mm) and was equal to 73% of the total water input (211 mm), including the snow water equivalent. The understory evapotranspiration reached 35% of the total evapotranspiration, and the interception evaporation was 15% of the gross precipitation. The understory evapotranspiration was high and the interception evaporation was low because the canopy was sparse and the *LAI* was low.

KEY WORDS Siberian larch forest, Energy and water balance, Canopy resistance, Land surface condition, GAME-Siberia

INTRODUCTION

Forests strongly affect water and energy cycles, and exist in different environments. It is thought that the effects of forest on the water and energy cycles and water budget vary according to the surrounding conditions.

In a humid, tropical region, like the Amazon, the latent heat flux is reported to be a relatively larger component of the energy cycle than the sensible heat flux (Shuttleworth et al., 1984, 1985, 1988). The magnitude of the latent heat flux sometimes exceeds the effective radiation when the canopy is wet (Shuttleworth et al., 1985). In a tropical monsoon forest, the latent heat flux consumes a large part of the available energy during the rainy season, and the Bowen ratio is below 1.0 (Pinker et al., 1980). Several General Circulation Model (GCM) simulations have predicted that tropical deforestation would increase air temperatures in this region (Shukla et al., 1990, Polcher and Laval, 1994).

There have been few investigations of the water and energy exchanges over forests in high latitude areas, compared with those of warm, humid areas. The effects of forest on the water and heat exchanges at high latitudes should differ from those in warm, humid regions, since high latitude areas are usually cool and dry. Recently, the BOREAS project was carried out in Northern Canada (Sellers et al., 1995). The seasonal change in the Bowen ratio over forests appeared “U”-shaped, and the minimum values, about 1.0, occurred in mid summer. The maximal values, about 2.0 - 3.0, occurred in early spring. A large part of the effective radiation was included in the sensible heat flux (Sellers et al., 1995). The daily evapotranspiration rates were usually 0.5 - 2.5 mm day^{-1}, and understory evapotranspiration was significant at 10 - 40% of the total evapotranspiration (Baldocchi et al., 1997). In other Canadian boreal forests, the daily mean evapotranspiration is reported to be 1.5 - 2.0 mm day^{-1} (Fitzjarrald and Moore, 1994, Lafleur, 1992, Amori and Wuschke, 1987). The NOPEX project was carried out in Sweden (Halldin et al., 1998). There, the daily mean evapotranspiration was 1.91 mm day^{-1} during the growing season, and 45 - 85% of this value consisted of transpiration (Grelle at al. 1997, Cienciala et al. 1997).

Differences in the transpiration rates of the dominant species of trees (larch, birch, and pine) have been reported in Siberia, and the maximal rates occurred in July. The transpiration rate was lower in a mature larch forest than in a young larch forest (Pozdnyakov, 1963, 1975, 1986, Maximov et al., 1996, Ivanov and Maximov, 1998). In Siberia, only a few short-term observations of water and energy exchanges have been carried out. These took place in central and eastern Siberian forests during mid summer (Kelliher et al., 1997, 1998). The Bowen ratios were 0.8 - 1.5 in the eastern Siberian larch

forest. These values are similar to those obtained in BOREAS. On the other hand, the ratios were 1.1 - 5.8 in a central Siberian pine forest. The daily mean evapotranspiration in the central and eastern Siberian forests was 1.7 and 1.9 mm day^{-1}, respectively. The evapotranspiration during the growing season estimated from these results was 169 mm, or 80% of the annual precipitation, for the larch forest, and 265 mm, or 90% of the annual precipitation, for the pine forest. Understory evapotranspiration was significant in both forests, at about 50%. GCM simulations predict that large-scale deforestation in high latitude regions will result in warming (Bonan et al., 1992, 1995, Thomas and Rowntree, 1992, Chalita and Treut, 1994).

The impact of forests on the water/energy cycles in high latitude regions will differ from those of tropical forests located in warm, humid regions. Little, however, is known about the seasonal variation in the components of the water and energy exchanges in Siberia based on long-term observations. Previous studies focusing on the water and energy exchanges during the growing season do not discuss the impact of snow cover. Forests, snow cover, and permafrost characterize the land surface of Siberia. This paper presents the properties of the seasonal variation in the energy and water balance, including not only the growing season but also snow-melt and leaf-fall seasons, in an eastern Siberian larch forest in one-dimensional scale, as they relate to land surface conditions.

METHODOLOGY

Site description and measurements

The study site is located at 62° 15' 18" N and 129° 37' 08" E, in the middle reaches of the Lena river. This is a continuous permafrost region, and the active layer is about 1.2 m deep in the larch forest. The altitude is 220 m a.s.l. The main species of tree is Dahurica larch (*Larix gmelinii*), with a stand density of 840 trees/ha. The mean stand height is 18 m. The value of the Plant Area Index (*PAI*) varied between 3.71 in the foliated season and 1.71 in the leafless season. The *PAI* was obtained from analysis of fisheye photos and was confirmed by litter fall observations. There was evergreen broad-leaved *Vactinium* understory vegetation 0.05 m high. Its leaf density is high, but the *PAI* (or *LAI*; the value of leaf area index) was not measured. The land surface has an incline of 1.6° towards the northeast, so the topography is quite flat.

A 32-m high observation tower was installed in the larch forest in the autumn of

1996, and preliminary observations began at the beginning of September 1996. More detailed observations were started in the middle of August 1997. The measurements recorded at the site are summarized in Table Ⅰ. Using automatic measurements, each variable was measured at exactly five-minute intervals, except wind speed, radiation, and ultrasonic anemometer measurements. Ventilated shelters covered the air temperature and humidity sensors. The wind speed was calculated from wind run measurements taken over five-minute periods with three-cup anemometers. The net all-wave radiation and four components of radiation were measured every minute, and the data loggers recorded average, maximum, and minimum radiation values. The average values are used in this study, and the sum of the four components of radiation is used as the net all-wave radiation. The upward and downward long-wave radiation was corrected using the sensed temperature at domes and sensor bodies. An ultrasonic anemometer operated every fifteen minutes and measured the three-dimensional wind speed and air temperature for 13.667 minutes at 10 Hz. A water vapor analyzer with a closed path operated intermittently at 10 Hz. These last devices were not operational for the entire period, because of difficulties with the power supply. The raw ultrasonic anemometer data for 13.667 minutes at 10 Hz, which was obtained every hour, were stored on the hard disk of a personal computer every five days.

Ground temperature was measured at 7 depths, 0, 0.1, 0.2, 0.4, 0.6, 0.8, and 1.2 m, and soil moisture was measured at 5 depths, 0.1, 0.2, 0.4, 0.6, and 0.8 m, with TDR sensors.

Precipitation was measured at an open site, 1 km south of the observation tower. The rain gauge was 40 cm in diameter and had an accuracy of 0.125 mm. Precipitation under the canopy was also measured near the tower. Stem flow was measured in four trees with different trunk diameters and canopy areas. Throughfall was measured using two 0.17×5.70 m troughs, and measurements were made just after each rainfall event.

Two plastic pans, 0.165 m in diameter and 0.075 m deep, were used to measure evapotranspiration from the forest floor. New undisturbed soil cores with vegetation were packed into the pans at the start of each experiment, and the pans were weighed every 2 hours in the daytime; they were not weighed at night. Measurements were carried out every 5 days.

Sap flow velocity was measured by the heat pulse method (Marshall, 1958, Yoshikawa et al., 1986) in order to estimate the rate of transpiration from the larch stand. The apparatus was installed on four larch trees with trunks of different diameters. Details of the trees used for sap flow measurements are summarized in Table II.

Data analysis

The energy balance above a forest canopy can be described as follows:

$$Rn = H + lE + G + J \quad (1)$$

where Rn is the net all-wave radiation, H is the sensible heat flux, lE is the latent heat flux, G is the ground heat flow, and J is the change in heat storage in the canopy layer. J should be taken into account for the analysis of diurnal variation. This study, however, discusses the daily energy balance, and J is ignored as the storage of heat during the day is canceled by energy released during the night.

The sensible heat flux is calculated by an eddy correlation method with the data obtained by the three-dimensional ultrasonic anemometer. The three dimensional coordinate axis is rotated to make the average vertical wind speed zero. The ultrasonic anemometer was inoperable at times because of electrical problems, such as powercuts and lightning. During these periods, a bulk transfer equation was used to obtain the sensible heat flux, written as follows:

$$H = \rho \cdot c_p \cdot C_H \cdot (T_s - T_Z) \cdot U_Z \quad (2)$$

where ρ is the density of air (kg m^{-3}), c_p is the specific heat of air under a steady pressure (J kg^{-1}), C_H is a bulk coefficient, T_s is the canopy temperature obtained by an infrared thermometer and T_Z and U_Z are the air temperature (°C) and the wind speed (m sec^{-1}) at a height of Z, respectively. The bulk coefficient was empirically decided by the relationship between the sensible heat flux obtained by the eddy correlation method and the product of ρ, cp, T_s-T_Z and U_Z.

In this study, the latent heat flux was calculated using equation (1). In addition, the latent heat flux was measured directly on some days using the gas analyzer with a closed path. The two values of the latent heat flux were comparable, and the latent heat flux calculated as the residual in equation (1) was corrected using the ratio of the latent heat flux measured directly to the residual value in equation (1).

Transpiration from the larch stand was estimated from sap flow measurement. First, the radial distribution of the sap flow velocity in the tree trunk was checked by the heat pulse method. Then, the volume of sap flow was estimated from these results using measurements of the actual water uptake from cut tree experiments (Roberts, 1977). Using this procedure, the relationship between the volume of sap flow and the sap flow velocity at the observation height was obtained for the four sample trees shown in Table II. Then, the relationship between the daily amount of sap flow and the diameter of the trunk

at breast height was obtained for the sample trees every day. The trunk diameters of all the trees in a 50 × 50m plot at the study site were measured in the summer of 1997. The total sap flow for all the trees was estimated from the relationship between the daily sap flow and trunk diameter. The total daily sap flow divided by the area of the plot, 2500 m^2, is the daily transpiration rate.

RESULTS AND DISCUSSION

Meteorological conditions in 1997 and 1998

Figure 1 shows the time series for the daily meteorological elements at the top of the tower in 1997 and 1998. During the 1997-98 winter, the batteries in the data loggers ran down, and we could not collect any data. The maximum net all-wave radiation occurred in June and was about 200 W m^{-2} in both years. The air temperature in the summer was higher in 1998 than in 1997. On the other hand, the relative humidity was higher in 1997 than in 1998. There was no remarkable difference in the wind speed between these two years.

Spectra of wind speed, air temperature, and water vapor density

Figures 2 and 3 show the power spectra and the cospectra of the vertical component of wind speed, air temperature, and water vapor density, respectively. According to the theory of turbulent flow, the spectra have a -2/3 slope in the inertial subrange. The power spectra of vertical wind speed and air temperature have a -2/3 slope in the inertial subrange (Figure 2 (a), (b)). The slope of water vapor density, on the other hand, is steeper than -2/3 and white noise is seen at high frequencies in these spectra (Figure 2 (c)). The data in the high frequency range, however, have little effect on the latent heat flux, because the cospectra in the same range are close to zero (Figure 3 (b)).

Nevertheless, the slopes of the power spectra are steeper than -2/3 and the water vapor densities are corrected using the response of the infrared sensor. The formula is given by the following equation:

$$C(i) = C_r(i) + \frac{1}{T} \cdot (C_r(i) - C_r(i-1)) / dt$$
$$T = V_{cel} / V_{flow} \qquad (3)$$

where $C(i)$ and $C_r(i)$ are the actual and recorded water vapor densities at time i, respectively, dt is the interval of measurement (sec), T is the response time of a sensor (sec), V_{cel} is the volume of a sensor cell (m^3), and V_{flow} is the absorbing rate of an air

sample (m^3 sec^{-1}). The power spectra and the cospectra corrected by the sensor response are shown in Figure 4. The power spectra in the high frequency range become larger and the slopes of the corrected spectra are close to -2/3 (Figure 4 (a)). On the other hand, the values of the cospectra corrected using the sensor response do not change significantly (Figure 4 (b)). This means that the difference between the estimated latent heat fluxes obtained from the raw data and the data corrected using the sensor response is small. The differences between the latent heat fluxes calculated using the raw and corrected data range from 0.35 - 10.5 W m^{-2} and the average value is 3.68 W m^{-2}.

The raw data for wind speed and air temperature with 10 Hz were not stored continuously during the entire study period and the differences between the latent heat fluxes obtained using the raw and corrected data were small, as mentioned above. Therefore, the latent heat flux calculated using the raw water vapor density data is regarded as the actual value.

Energy balance

The bulk coefficient had to be determined to estimate the sensible heat flux when the ultrasonic anemometer was not functioning. Using Equation (2), the bulk coefficient can be calculated from the sensible heat flux obtained using the 3-dimensional ultrasonic anemometer and the meteorological variables. The slope in this relationship gives the bulk coefficient. Under unstable conditions, it was possible to use a linear relationship, and the value of the bulk coefficient was 0.017. On the other hand, there was no significant relationship under stable conditions. The bulk coefficient was strongly affected by atmospheric stability and decreased exponentially with an increase in the stability. The bulk coefficient can be represented by the following equations:

$$\begin{aligned} C_H &= 0.017 \text{.....} \textit{Unstable...Condition} \\ C_H &= e^{(-4.1-4.5Rb)} + 0.0005 \text{.....} \textit{Stable...Condition} \end{aligned} \qquad (4)$$

where *Rb* is the Bulk Richardson number.

The agreement between the two values for the sensible heat flux was generally good: H_{eddy} = 0.909H_{bulk} + 18.9 with r^2 = 0.75 for 1900 hourly data. The standard deviation of the error was 45.5 W m^{-2}. The sensible heat flux calculated by the bulk method was used when the ultrasonic anemometer was inoperable.

The eddy correlation method for latent heat flux could only be used intermittently, so the latent heat flux, *lE*, was calculated using Equation (1), substituting the values for the net all-wave radiation, *Rn*, ground heat flow, *G*, and sensible heat flux, *H*. The latent

heat flux calculated using Equation (1) was compared with those obtained by the eddy correlation method. Table III shows the ratios of the latent heat flux obtained by the eddy correlation method to that calculated using Equation (1). The ratio varied with the canopy conditions and increased with the foliage density. For the actual values, the latent heat flux calculated from Equation (1) is corrected by the following equation.

$$lE_C = \alpha \cdot lE \qquad (5)$$

where lE_C is the corrected latent heat flux, lE is the latent heat flux determined as the residual for Equation (1), and α is the coefficient shown in Table III.

The energy budget was not completely closed at the observation site on a one-dimensional scale. The relationship between the effective radiation, $Rn - G$, and the sum of turbulent fluxes was described by:

$$H + lE_C = 0.752 \cdot (Rn - G) \qquad (6)$$

Similar differences of 60 - 90% have been reported elsewhere (Verma et al., 1986, Lee and Black, 1993, Kelliher et al., 1997, Constantin et al., 1998). The reasons for the energy imbalance are as follows. First, the ground heat flow is underestimated. The daily ground heat flow fluctuated between 10 - 30 W m^{-2} after the snow melt season. This value does not seem sufficient to cause thawing to depths of up to 120 cm. Second, the latent heat flux is underestimated. As shown in Figure 2, the slope of the relationship between the frequency and the power spectrum of water vapor density is steeper than -2/3. Air sampling and sensor response may produce some of this underestimation, but the loss due to these causes does not seem to be enough to close the energy balance as mentioned in the previous section. The third reason for the imbalance is the effect of the average flow for the vertical component of wind speed. The extent of vertical wind flow is reported to result in underestimating the turbulent energy fluxes, although the average vertical wind velocity becomes zero due to the rotation of the three-dimensional wind speed data (Lee, 1998). Future studies will resolve the reasons for the non-closure of the 1-D energy balance at this site.

Figure 5 shows the seasonal variation in the daily values of the energy balance components ((a) and (b)) and the Bowen ratio (c) during the warm season in 1998. The surface condition during this period is also shown in this figure by bars. These figures only show the time series for a dry canopy. The latent heat flux did not increase during early May, in the snowmelt season, although the soil surface was very wet because of

water from melting snow. Then, the latent heat flux increased rapidly, when larch trees began to open their leaves, because transpiration occurred at this time. Figure 6 shows the time series for soil temperature. The leaves began to open in the larch stand when the thaw reached a depth of 10 - 20 cm. At least 80% of the roots, especially the thin roots, are distributed in the top 20 cm of soil, and the water uptake from this shallow layer of soil was important for the changes in the water and energy balances. In contrast, the sensible heat flux peaked in the middle of May when trees did not have leaves and the soil surface was snow-free. Although the net all-wave radiation increased, the sensible heat flux decreased from the leaf-opening season, in early June, to the foliated season, in the middle of July, because the latent heat flux increased. Snowmelt did not directly affect the energy balance above the canopy and the latent heat flux did not change during the snowmelt season just after ablation of the snow cover. Plant physiological activity, on the other hand, was important for the energy balance. Previous studies focused mainly on the growing season, so the differences between the effects of snow and plant physiological processes on the energy balance were not known. These results show the importance of plant effects on the water and energy exchanges.

The seasonal variation in the Bowen ratio was clearly “U”-shaped (Figure 5 (c)). The same seasonal variation in the Bowen ratio has been observed in Canadian boreal forests (Sellers et al., 1995) and in a snowy Japanese pine forest (Suzuki et al., 1999). At the study site, the Bowen ratio was around 1.0 during the summer, similar to values measured in other boreal forests (Sellers et al., 1995, Kelliher et al., 1997). On the other hand, the Bowen ratio in the spring and autumn was very high. The Bowen ratio at the site was 10 - 25 in the early spring in 1998, before the leaves opened, much higher than the values obtained in other forests. The elevation of the sun is high at this time. Moreover, the albedo above the canopy was not high (0.22 - 0.27), even when the larch stand had no foliage and the forest floor was snow-covered. After snowmelt, while there was still no foliage, the albedo was 0.11 - 0.13. The larch stand was unable to take up water because the trees were leafless and the soil was frozen. A large part of the available energy is converted to sensible heat flux in early spring, and the warming effect on the atmosphere is much stronger in a Siberian forest than in North American forests, judging by the magnitude of the Bowen ratio.

Aerodynamic resistance and canopy resistance for a big leaf model, and environmental variables

This paper uses parameters in a big leaf model, Penman-Monteith formula, to analyze the characteristics of water and energy exchanges above the canopy. The

aerodynamic and canopy resistance limit the water and energy exchanges in a big leaf model. The aerodynamic resistance, r_a, was calculated from the roughness length and the zero plane displacement, which were estimated from the friction velocity determined with the ultrasonic anemometer and the wind speed profiles in near neutral conditions (Ohta et al., 1999). The aerodynamic resistance, r_a, can be written as:

$$r_a = \frac{\ln((z-d)/z_0)^2}{\kappa^2 U(z)} = \frac{1}{C_H \cdot U(z)} \qquad (7)$$

where z_0 is the roughness length, d is the zero plane displacement, κ is the Von Kalman's constant, and $U(z)$ is the wind speed at a height of z. Table IV shows the values of z_0 and d for different canopy conditions. There were no remarkable differences in these parameters, although *PAI* was smaller in the leafless season than in the foliated season. The canopy is quite sparse at the site, even when the larch stand has leaves, so the leaves did not strongly affect the aerodynamic parameters. These parameters did not change significantly with canopy condition (foliated or leafless) in a very dense oak forest with 3,000 trees ha^{-1} (Dolman 1986). On the other hand, they were dramatically different for leafless and foliated canopies in an ash forest with 800 trees ha^{-1} (Ohta et al., 1999). These results suggest that the aerodynamic parameters are not only controlled by the density of leaves, i.e., the *LAI*, but also by the spatial distribution of canopy components.

The canopy resistance, r_c, was calculated using the Penman-Monteith formula (Monteith and Unsworth, 1973) written as:

$$lE = \frac{\Delta(Rn-G) + \rho \cdot c_p \cdot (e_s(T_a) - e_a)/r_a}{\Delta + \gamma(1 + r_c/r_a)} \qquad (8)$$

where Δ is the slope of the saturated water vapor pressure versus temperature curve when the air temperature is T_a, $e_s(T_a)$ is the saturated water vapor pressure when the air temperature is T_a (hPa), e_a is the observed water vapor pressure (hPa), and γ is the psychrometer constant. The canopy resistance usually varies diurnally, and is low at midday and high in the morning and evening. In this study, the daily mean canopy resistance is defined as the average value when the net all-wave radiation exceeded 150 W m^{-1}.

Another parameter, the evapotranspiration efficiency, β, is also used to assess evapotranspiration characteristics. The evapotranspiration efficiency is defined as:

$$\beta = \frac{r_a}{r_a + r_c} \tag{9}$$

When the canopy is wet, the canopy resistance, r_c, is 0 and the evapotranspiration efficiency under a wet canopy is 1.0.

Figure 7 shows the time series for the daily mean resistance. The canopy resistance ranged widely between 100 - 1500 sec m^{-1}, while the aerodynamic resistance was very low, 6 - 20 sec m^{-1}. This means that evapotranspiration from the larch forest was poorly coupled with the aerodynamic resistance. A similar result was obtained in a Canadian forest (Baldocchi et al., 1997).

The canopy resistance increased with the saturation deficit when the larch stand had foliage; there was no remarkable relationship during the leafless season (Figure 8(a)). Consequently, when the larch stand had foliage, the evapotranspiration efficiency decreased exponentially as the saturation deficit increased, (Figure 8(b)). The minimum canopy resistance was 100 sec m^{-1}, which corresponded to a canopy conductance of 10 mm sec^{-1}. This is similar to results obtained in another Siberian larch forest (Kelliher et al., 1997). The maximum canopy conductance was 15 - 30 mm sec^{-1} (or a canopy resistance of 30 - 67 sec m^{-1}) in forests located at 40°N - 50°N, and the mean value was 19.7 mm sec^{-1} (Kelliher et al., 1995). The evapotranspiration efficiency became 0.02 - 0.05 asymptotically as the saturation deficit increased. The minimum evapotranspiration efficiency was 0.2 in a Japanese red pine forest during the growing season (Suzuki et al., 1999). The values of r^2 in the relationship between the saturation deficit and the canopy resistance for the foliated and leaf-fall seasons were 0.445 and 0.666, respectively. These results indicate that the saturation deficit strongly restricted evapotranspiration in the Siberian larch forest. The canopy resistance was lower in the foliated season than in the leaf-fall season (Figure 8(a)), which implies that the senescence of leaves affects the characteristics of the water and energy exchanges.

Figure 9 shows the relationship between solar radiation and the canopy resistance. The canopy resistance increased with the radiation for the leaf-fall season, although the relationship was not as significant as the relationship between the saturation deficit and the evapotranspiration efficiency. The values of r^2 in the relationship between the solar radiation and the canopy resistance for the foliated and leaf-fall seasons were 8.50×10^{-5} and 0.162, respectively, as these relationships were approximated by linear relationships. These values indicate that their correlation was low. The relationship between air temperature and the canopy resistance is shown in Figure 10. The canopy resistance had a minimum value at 7 - 10 °C. The relationship during the leafless period was not clear.

The values of r^2 in the relationship between the air temperature and the canopy resistance for the foliated and leaf-fall seasons were 0.449 and 0.357, respectively.

Surface soil moisture effects on the canopy resistance and evapotranspiration efficiency were also examined, but these parameters were poorly coupled with soil moisture at a depth of 20 cm. The value of r^2 in the relationship between the soil moisture at 20 cm depth and the canopy resistance was 0.0942, as the correlation was approximated by a linear relationship. Soil moisture was an important factor for determining the canopy conductance in a central Siberian pine forest (Kelliher et al., 1997). On the other hand, there was no significant relationship between soil moisture and the canopy conductance in a Canadian boreal forest (Baldocchi et al., 1997). The influence of soil moisture on the canopy resistance of a Siberian larch forest was also not significant.

According to these results, the saturation deficit affects the canopy resistance and the evapotranspiration efficiency most strongly and air temperature is of secondary importance in controlling the canopy resistance.

Water balance

The total precipitation from 21 April 1998 to 7 September 1998 was 106 mm and the water equivalent of the snow cover was 105 mm just before the snowmelt, giving a total water input into the ecosystem during the warm season of 211 mm.

Sublimation evaporation from the snow surface was approximately 11% of the water equivalent of the snow cover from 21 April to 15 May 1998 (Hashimoto et al., 1999). The amount of evaporation estimated from the latent heat flux was 6.9 mm for this period, and the two values agreed well. During the snow-covered season, evapotranspiration from the forest resulted from the sublimation of snow.

In order to calculate the transpiration rate, the experimental relationship between the measured sap flow and trunk diameter at breast height is given by:

$$V = a \cdot DBH^{\,b} \tag{10}$$

where V is the amount of sap flow (liters/day), DBH is the diameter of the tree trunk at breast height (cm), and a and b are coefficients. This relationship was determined daily for the four sample trees, as described in the “Methodology” section. The values of a and b were 0.0129 - 0.508 and 1.23 - 2.10, respectively, and r^2 in the relationship between the trunk diameter and the amount of sap flow was 0.597 - 0.982. The time series for total

evapotranspiration from the forest calculated from the latent heat flux and transpiration estimated from sap flow measurements, is shown in Figure 11. The maximum evapotranspiration rate, 2.9 mm day^{-1}, occurred at the beginning of July. On the other hand, the transpiration rate reached a maximum value of 1.7 mm day^{-1}, in the middle of June. The average evapotranspiration rate was 1.16 mm day^{-1} during the observation period. During the growing season, from 1 June to 31 August, the average evapotranspiration and transpiration rates were 1.49 and 1.1 mm day^{-1}, respectively.

The total evapotranspiration from the forest consists of the transpiration from larch trees and the understory evapotranspiration. The difference between the total evapotranspiration calculated from the latent heat flux above the canopy and the transpiration estimated by sap flow velocity shown in Figure 11 gives the understory evapotranspiration (except for rainy days). Figure 12 shows the time series for the understory evapotranspiration, obtained from the difference between evapotranspiration from the forest and transpiration from the trees and from the pan measurements, and the surface soil moisture content. The two seasonal patterns of understory evapotranspiration agree well. The surface soil moisture decreased monotonously from the beginning of June to the end of August. On the other hand, the understory evapotranspiration fluctuated during this period, so there was no remarkable relationship between the understory evapotranspiration and the surface soil moisture content. From 4 June to 7 September, the amount of understory evapotranspiration calculated from the difference between evapotranspiration from the forest and the trees was 45.2 mm, which equaled 35% of the total evapotranspiration. This ratio is high compared with values obtained for forests in warm, humid regions with dense canopies. On the other hand, the percentage of understory evapotranspiration to the total evapotranspiration at this site is similar to previously reported values (Kelliher et al., 1997, 1998, Baldocchi et al., 1997). The percentages of understory evapotranspiration were not as high (13 - 15%) in pine and spruce forests in Sweden because of the high *LAI* (Lindroth, 1985, Grelle et al., 1997). The understory evapotranspiration is not negligible in Siberian forests.

The maximum stem flow was only 0.07% of the gross amount of precipitation during each event, so stem flow could be neglected in the water balance. On the other hand, throughfall was 78.5 - 89.2% of the gross amount of each precipitation event. Therefore, the interception evaporation was about 15% of the precipitation. This value is lower than in the Swedish pine-spruce stand (Grelle et al., 1997), because the canopy is sparser in the Siberian larch forest than in the Swedish pine-spruce forest.

From these results, the water balance from 21 April 1998 to 7 September 1998 can

be summarized as follows: Total water input was 211 mm, including the water equivalent of the snow cover (105 mm). Evapotranspiration from the forest was 151 mm, and the understory evapotranspiration was equal to 35% of the total evapotranspiration. The interception evaporation, 16 mm, was 15% of the gross precipitation at the open site. The total evapotranspiration exceeded the total precipitation, and snowmelt water compensated for this deficit.

CONCLUDING REMARKS

The energy and water exchanges in a Siberian larch forest were measured. The following new insights were gained in this study:

(1) The latent heat flux increased rapidly as the larch stand began to foliate, and the sensible heat flux dropped at the same time. The latent heat flux peaked at the beginning of July and decreased gradually after the middle of August. Melting snow did not have a direct effect on the changes in the energy balance above the canopy, and plant activity was important for the seasonal variation in the water and energy exchanges.

(2) The seasonal variation in the Bowen ratio was clearly “U”-shaped. The minimum values, about 1.0, occurred from the middle of June to the middle of July. The Bowen ratio was quite high in the early spring, and reached 10 -25.

(3) The canopy resistance far exceeded the aerodynamic resistance, and it fluctuated widely. The value of r_{cmin} was 100 sec m^{-1}. The saturation deficit and air temperature controlled the canopy resistance, and the saturation deficit strongly limited the canopy resistance. The canopy resistance was higher during the leaf-fall season than in the foliated season, as the saturation deficit had the same value. This suggests that the senescence of the foliage also affects the canopy resistance.

(4) The 151 mm of evapotranspiration from the forest was 73% of the total input water, including melt water, from 21 April to 7 September 1998. This value exceeds the amount of precipitation during this period. The magnitude of the understory evapotranspiration was not negligible, and was 35% of the total evapotranspiration. The interception evaporation was equal to 15% of the precipitation.

ACKNOWLEDGMENTS

This study was carried out as part of GAME (GEWEX Asian Monsoon Experiment)-Siberia. The authors would like to thank Professor T. Yasunari, of

University of Tsukuba, for giving us the opportunity to investigate hydro-meteorological processes in Siberia. We would like to thank Professor B. Ivanov, Director of the Institute for Biological Problems of Cryolithozone, for his kind collaboration in this work. The authors would also like to thank all the members of the GAME-Siberia project for their cooperation and discussions. We would like to thank Dr. I. Tamagawa, Associate Professor, of Gifu University, for his useful comments on the spectrum analysis. Finally, the authors would like to thank the editor and the reviewers for their many useful and constructive comments.

This study was financially supported by Grants-in-Aid of Scientific Research (No.11691124, No.11201206 and No.11201201) from the Japanese Ministry of Education, Sports and Culture.

REFERENCES

Amiro BD, Wuschke EE. 1987. Evapotranspiration from a boreal forest drainage basin using an energy balance/eddy correlation technique. Boundary-Layer Meteorology. 38: 125-139.

Baldocchi DD, Vogel CA, Hall B. 1997. Seasonal variation of energy and water vapor exchange rates above and below a boreal jack pine canopy. Journal of Geophysical Research. 102. D24: 28939-28951.

Bonan GB, Pollard D, Thompson SL. 1992. Effects of boreal forest vegetation on global climate. Nature. 359: 716-718.

Bonan GB, Chapin III FS, Thompson SL. 1995. Boreal forest and tundra ecosystems as components of the climate system. Climatic Change. 29: 145-167.

Chalita S, Treut HL. 1994. The albedo of temperate and boreal forest and the northern hemisphere climate--a sensitivity experiment using the LMD GCM. Climate Dynamic. 10: 231-240.

Cienciala E, Kucera J, Lindroth A, Cermak J, Grelle A, Halldin S. 1997. Canopy transpiration from a boreal forest in Sweden during a dry year. Agricultural and Forest Meteorology. 86: 157-167.

Constantin J, Inclan MG, Raschendorfer M. 1998. The energy budget of a spruce forest: field measurements and comparison with the forest-land-atmosphere model (FLAME). Journal of Hydrology. 212-213. 22-35.

Dolman AJ. 1986. Estimate of roughness length and zero plane displacement for a foliated and non-foliated oak canopy. Agricultural and forest Meteorology. 36: 241-248.

Fitzjarrald DR, Moore KE. 1994. Growing season boundary layer climate and surface exchanges in a subarctic lichen woodland. Journal of Geophysical Research. 99. D1: 1899-1917.

Grelle A, Lundberg A, Lindroth A, Moren A-S, Cienciala E. 1997. Evaporation components of a boreal forest: variations during the growing season. Journal of Hydrology. 197: 70-87.

Halldin S, Gottschalk L, Griend AA, Gryning S-E, Heikinheimo M, Hogstrom U, Jochum A, Lundin L-C. 1998. NOPEX-- a Northern Hemisphere climate processes land surface. Journal of Hydrology. 212-213: 172-187.

Hashimoto T, Ohta T, Toba T, Maximov TC, Kononv A. 1999. Heat balance characteristics of snow pack during snowmelt season in a boreal forest over the eastern Siberia. Proceedings of "Third International Scientific Conference on the Global Energy and Water Cycle". June, 1999. Beijing: 264-265.

Ivanov BI, Maximov TC. 1998. The role of permafrost ecosystem in balance of greenhouses gases. Siberian Ecological Journal. 3-4. 233-236.

Kelliher FM, Leuning R, Raupach MR, Schulze E-D. 1995. Maximum conductances for evaporation from global vegetation types. Agricultural and Forest Meteorology. 73: 1-16.

Kelliher FM, Hollinger DY, Schulze E-D, Vygodskaya NN, Byers JN, Hunt JE, McSeveny TM, Milukova I, Sogatchev A, Varlargin A, Ziegler W, Arneth A, Bauer G. 1997. Evaporation from an eastern Siberian larch forest. Agricultural and Forest Meteorology. 85: 135-147.

Kelliher FM, Lioyd J, Arneth A, Byers JN, McSeveny TM, Milukova I, Grigoriev S, Panfyorov M, Sogatchev A, Varlargin A, Ziegler W, Bauer G, Schulze E-D. 1998. Evaporation from a central Siberian pine forest. Journal of Hydrology. 205: 279-296.

Lafleur PM. 1992. Energy balance and evapotranspiration from a subarctic forest. Agricultural and Forest Meteorology. 58: 163-175.

Lee X, Black TA. 1993. Atmospheric turbulence within and above a Douglas-fir stand - Part II: eddy fluxes of sensible heat flux and water vapor. Boundary-Layer Meteorology. 64: 369 - 389.

Lee X. 1998. On micrometeorological observations of surface-air exchange over tall Vegetation. Agricultural and Forest Meteorology. 91: 39-49.

Lindroth A 1985. Seasonal and diurnal variation of energy budget components in coniferous forests. Journal of Hydrology. 82: 1-15.

Marshall DC 1958. Measurement of sap flow in conifers by heat transport. Plant

Physiology. 33: 385-396.

Maximov TC, Maximov AP, Kononov AV. 1996. Balance of Carbon dioxide and water in permafrost ecosystem of Yakutia. Proceedings of "The third international study conference on GAME", Cheju Island: 104-111.

Monteith JL, Unswoth MH. 1990. Steady state heat balance (I) water surface and vegetation Principles of environmental physics. Edward Arnold: London; 177 - 198.

Ohta T, Suzuki K, Kodama Y, Kubota J, Kominami Y, Nakai Y. 1999. Characteristics of the heat balance above the canopies of evergreen and deciduous forests during the snowy season. Hydrological Processes. 13: 2383 - 2394.

Pinker RT, Thompson OE, Eck TF. 1980. The energy balance of a tropical evergreen forest. Journal of Applied Meteorology. 19: 1341-1350.

Polcher J, Laval K. 1994. The impact of African and Amazonian deforestation on tropical climate. Journal of Hydrology. 155: 389-405.

Pozdnyakov LK. 1963. Hydro-climate regime of larch forest in Central Yakutia. Science: Moscow; 146p (in Russian)

Pozdnyakov LK. 1975. Larch daurica. Science: Moscow; 130p. (in Russian)

Pozdnyakov LK. 1986. Permafrost Dendrology. Science: Novosibirsk; 192p. (in Russian)

Roberts J. 1977. The use of tree-cutting in the study of the water relations of mature *Pinus sylvestris L*. Journal of Experimental Botany. 28: 751-767.

Sellers P, Hall F, Margolis H, Kelly B. Baldocchi D, Hartog GD, Cihlar J, Ryan MG, Goodison B, Crill P, Ranson KJ, Lettenmaier D, Wickland DE. 1995. The boreal ecosystem-atmosphere study (BOREAS): An overview and early results from the 1994 field year. Bulletin of American Meteorological Society. 76: 1549-1577.

Shulka J, Nobre C, Sellers P. 1990. Amazon deforestation and climate change. Science. 247: 1322-1325.

Shuttleworth WJ, Gash JHC, Lloyd CR, Moore CJ. 1984. Eddy correlation measurements of energy partition for Amazonia. Quarterly Journal of the Royal Meteorological Society. 110: 1143-1162.

Shuttleworth WJ, Gash JHC, Lloyd CR, Moore CJ, Roberts J. 1985. Daily variation of temperature and humidity within and above Amazonian forest. Weather. 40: 102-108.

Shuttleworth WJ. 1988. Evaporation from Amazonian rainforest. Proceedings of Royal Society London. B233: 321-346.

Suzuki K, Ohta T, Miya H, Yokota S. 1999. Seasonal variation of heat balance components over a Japanese red pine forest in snowy northern Japan. Hydrological Processes. 13: 2409 - 2421.

Thomas G, Rowntree T. 1992. The boreal forests and climate. Quarterly Journal of the

Royal Meteorological Society. 118: 469-497.

Verma SB, Baldocchi DD, Anderson DE, Matt DR, Clement RJ. 1986. Eddy fluxes of CO2, water vapor and sensible heat flux over a deciduous forest. Boundary-Layer Meteorology. 36: 71-91.

Yoshikawa K, Ogino K, Maiyus M. 1986. Some impacts of sap flow rate of tree species in a tropical rain in west Sumatra. In : Diversity and dynamics of plant life in Sumatra (ed. Hatta M.), pp. 45-59. Sumatra Nature Study (Botany), Kyoto.

Captions of Figures and Tables

Figure 1 Time series for the daily meteorological elements at the top of the observation tower. (a) Time series of the net all-wave radiation and the four radiative components. *Rn*: net all-wave radiation, *Sd*: downward short-wave radiation, *Su*: upward short-wave radiation, *Ld*: downward long-wave radiation, *Lu*: upward long-wave radiation. (b) Time series of the air temperature and the relative humidity. *Ta*: air temperature, *RH*: relative humidity. (c) Time series of wind speed.

Figure 2 Power spectra of vertical wind speed (a), air temperature (b), and water vapor density (c).

Figure 3 Cospectra of vertical wind speed - air temperature (a) and vertical wind speed-water vapor density (b).

Figure 4 Power spectra (a) and cospectra (b) obtained from the raw data and the corrected data for water vapor density. Bold lines show the values calculated using the corrected data, and fine lines show the values calculated using the raw data.

Figure 5 Time series for the daily net all-wave radiation and the ground heat flow (a), the sensible heat flux and the latent heat flux (b), and the Bowen ratio (c). The energy balance components and the Bowen ratio indicated in this figure are for a dry canopy only.

Figure 6 Time series for the soil temperature.

Figure 7 Time series for the aerodynamic and canopy resistances. These resistances were not calculated for rainy days.

Figure 8 Relationship between the canopy resistance (a), the evapotranspiration efficiency (b) and the saturation deficit above a dry canopy.

Figure 9 Relationship between the canopy resistance and the incoming solar radiation above a dry canopy.

Figure 10 Relationship between the canopy resistance and the air temperature above a dry canopy.

Figure 11 Time series for the daily total evapotranspiration from the forest and daily transpiration from the larch trees only. The daily evapotranspiration and the daily transpiration were calculated from the latent heat flux and the sap flow velocity, respectively.

Figure 12 Time series for the understory evapotranspiration (a) based on the difference between total evapotranspiration and transpiration (●), and pan measurements (○) , and surface soil moisture content (b).

Table I

Observed items	Sensor type	Data logging
Short-wave radiation (upwards and downwards) above the canopy and the forest floor	CM-6F; Kipp & Zonen	Logging: 1 minute. Record: 5 minutes average value
Long-wave radiation (upwards and downwards) above the canopy and the forest floor	MS-201F; Eiko	Logging: 1 minute. Record: 5 minutes average value
Net all-wave radiation above the canopy and the forest floor	Q7; REBS	Logging: 1 minute. Record: 5 minutes average value
Air temperature and relative humidity 2 levels above the canopy; 31.4, 24.6 m 2 levels under the canopy; 5.7, 1.8 m	HMP-35D Vaisala	Logging and record: 5 minutes
Wind speed (wind run) 3 levels above the canopy; 32.0, 27.0, 24.8 m 3 levels under the canopy; 14.9, 5.7, 1.9 m	AC-750; Makino	Record: 5 minutes average value
Canopy surface temperature	4000-4GL; Everest	Logging and record: 5 minutes
Sensible heat flux at the top of tower (32 m height)	DA-600; Kaijo	Record: 13.67 minutes average value
Latent heat flux at the top of tower (32 m height)	LI-6262; Li-COR	Record: 13.67 minutes average value
Ground heat flow 0.05 m depth	MF-81; Eiko	Logging and record: 5 minutes
Ground temperature 7 depths; 0, 0.1, 0.2, 0.4, 0.6, 0.8, 1.2 m	TS101; Hakusan Kougyo	Logging and record: 5 minutes
Soil moisture content 5 depths; 0.1, 0.2, 0.4, 0.6, 0.8 m	P2 sensor; TRIME IMKO	Logging and record: 5 minutes
Throughfall	Manual observation	every precipitation event
Stem flow	Manual observation	every precipitation event

Table II

Tree used for sap flow measurement	Tree height (m)	Diameter of tree trunk at breast height (m)	Area of tree canopy (m^2)	Height of heat pulse sensor (m)
A	14.7	0.121	6.7	1.0
B	16.1	0.161	9.5	1.0
C	18.9	0.308	28.5	1.0
D	16.3	0.156	5.9	1.0

Table III

Canopy condition	Ratio of latent heat flux obtained by the eddy correlation method to that obtained by the energy balance method
Leafless canopy	0.316
Opening leaves	0.406
Foliated canopy	0.533

Table IV

Canopy condition	z_0 (m)	d (m)
Leafless canopy	2.31	5.51
Foliated canopy	2.58	6.24

Figure 1

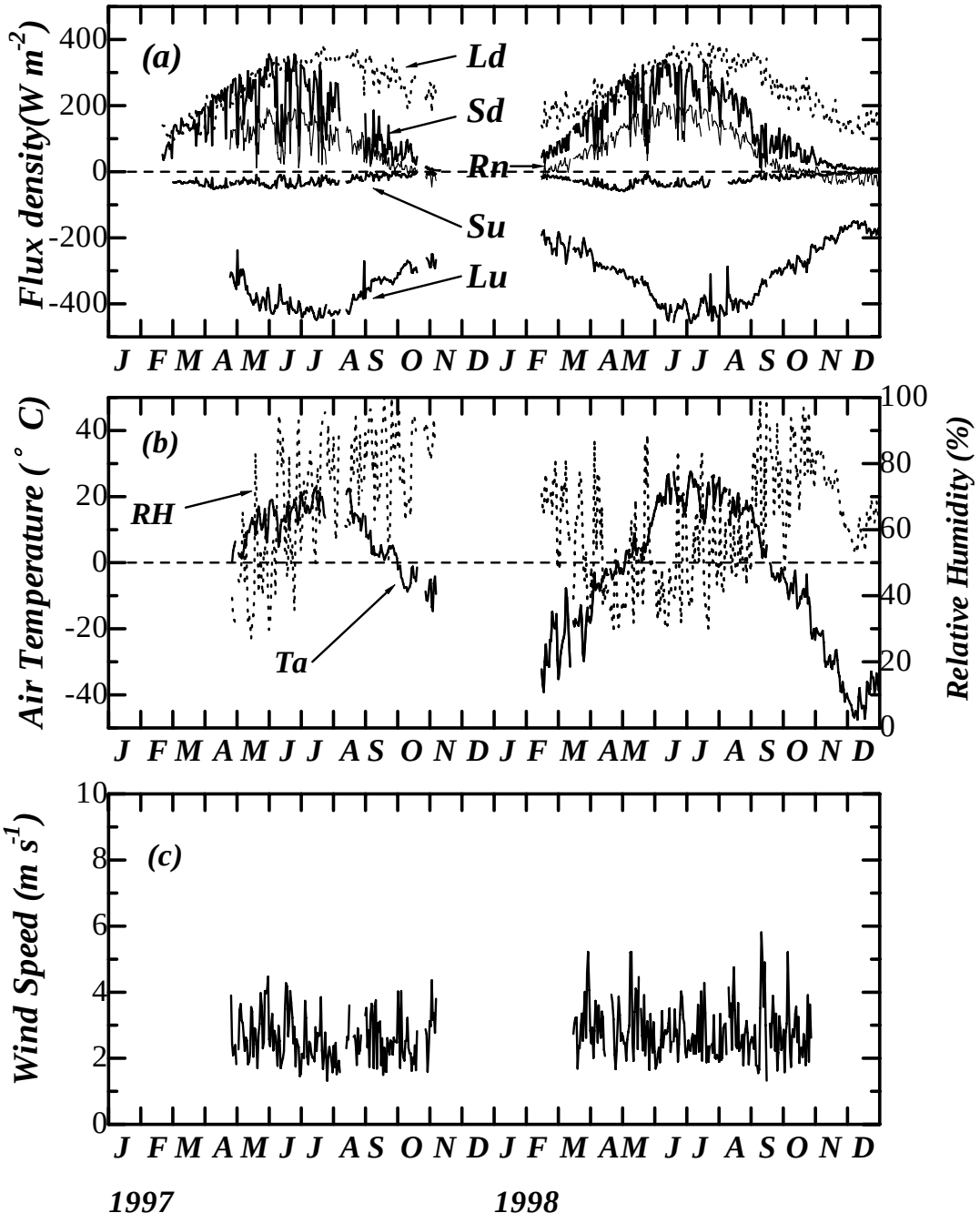
(a)
Ld
Sd
Rn
Su
Lu
Flux density(W m-2)
400
200
0
-200
-400
J F M A M J J A S O N D J F M AM J J A S O N D
(b)
RH
Ta
Air Temperature (° C)
40
20
0
-20
-40
100
80
60
40
20
0
Relative Humidity (%)
J F M A M J J A S O N D J F M AM J J A S O N D
(c)
Wind Speed (m s-1)
10
8
6
4
2
0
J F M A M J J A S O N D J F M AM J J A S O N D
1997
1998

Figure 2

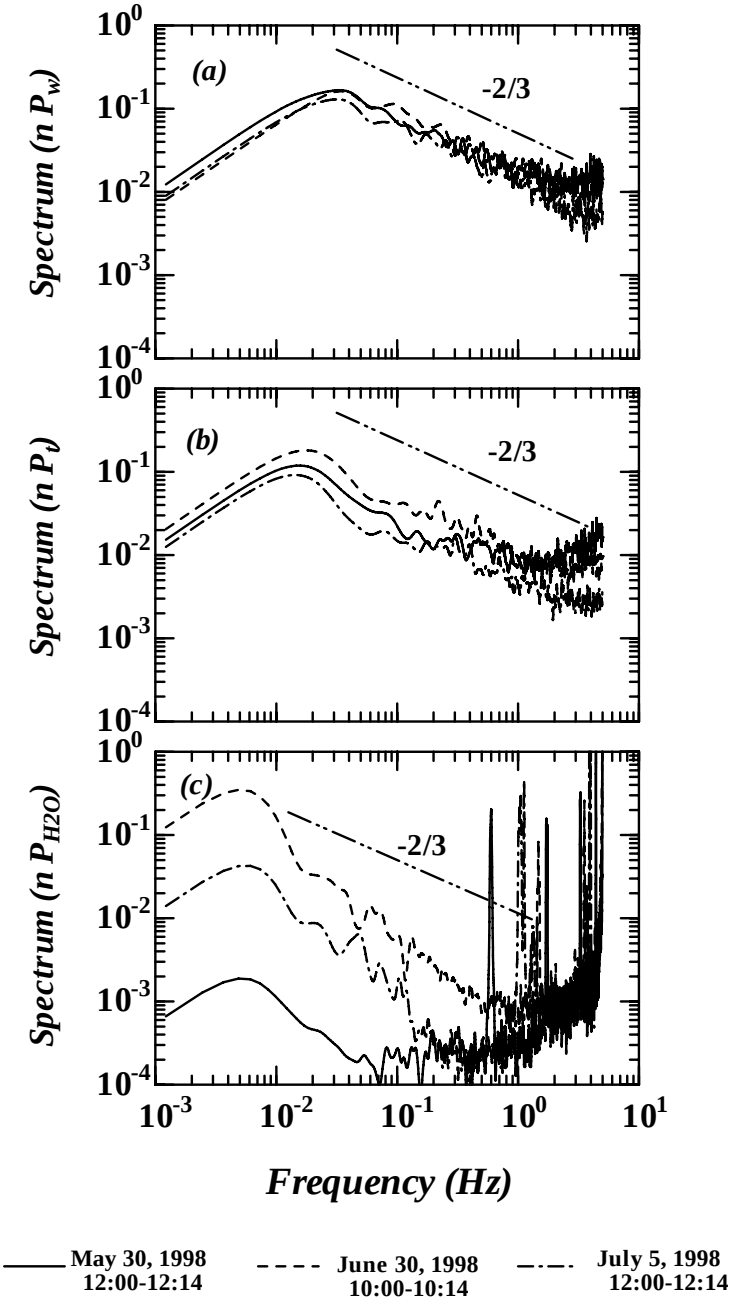
(a)
-2/3
Spectrum (n P_w)
(b)
-2/3
Spectrum (n P_t)
(c)
-2/3
Spectrum (n P_{H2O})
Frequency (Hz)
May 30, 1998 12:00-12:14
June 30, 1998 10:00-10:14
July 5, 1998 12:00-12:14

Figure 3

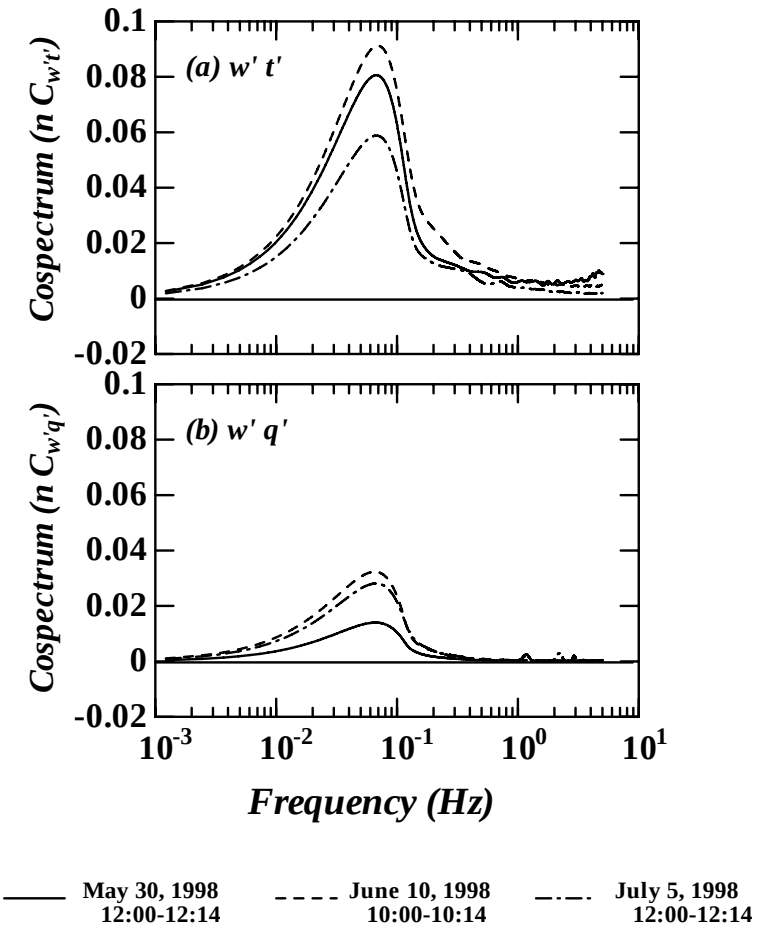
0.1
0.08
0.06
0.04
0.02
0
-0.02
(a) w' t'
Cospectrum (n Cw't')
(b) w' q'
Cospectrum (n Cw'q')
10-3
10-2
10-1
100
101
Frequency (Hz)
May 30, 1998
12:00-12:14
June 10, 1998
10:00-10:14
July 5, 1998
12:00-12:14

Figure 4

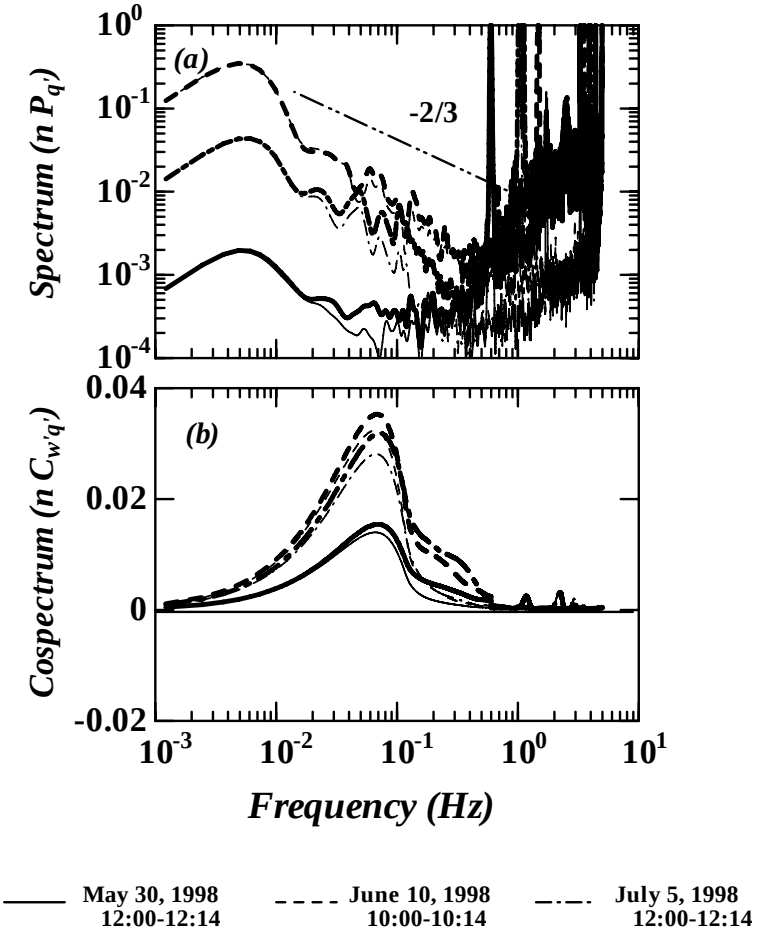
(a)
-2/3
Spectrum (n $P_{q'}$)
(b)
Cospectrum (n $C_{w'q'}$)
Frequency (Hz)
May 30, 1998 12:00-12:14
June 10, 1998 10:00-10:14
July 5, 1998 12:00-12:14

Figure 5

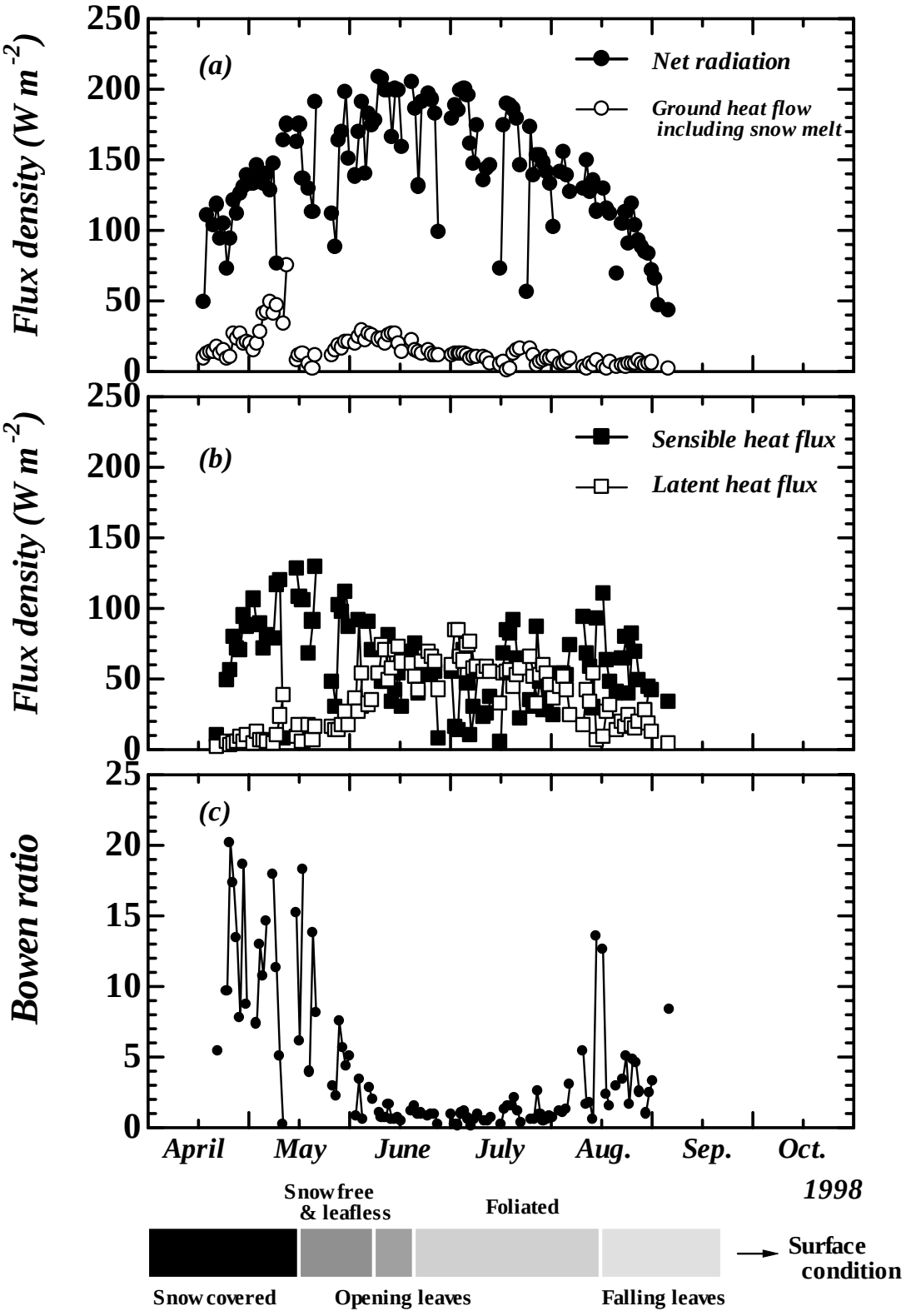
(a)
Net radiation
Ground heat flow including snow melt
Flux density (W m-2)
250
200
150
100
50
0
(b)
Sensible heat flux
Latent heat flux
Flux density (W m-2)
250
200
150
100
50
0
(c)
Bowen ratio
25
20
15
10
5
0
April
May
June
July
Aug.
Sep.
Oct.
1998
Snow free & leafless
Foliated
Surface condition
Snow covered
Opening leaves
Falling leaves

Figure 6

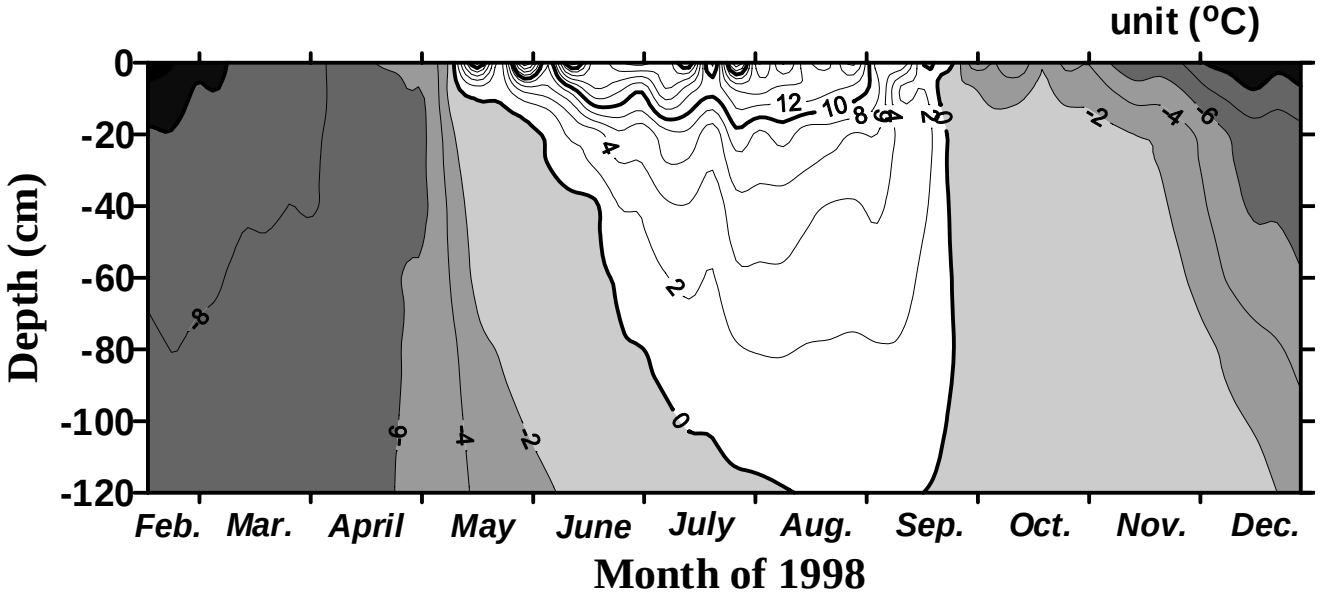
unit (°C)
Depth (cm)
0
-20
-40
-60
-80
-100
-120
12
10
8
6
4
2
0
-2
-4
-6
-8
Feb.
Mar.
April
May
June
July
Aug.
Sep.
Oct.
Nov.
Dec.
Month of 1998

Figure 7

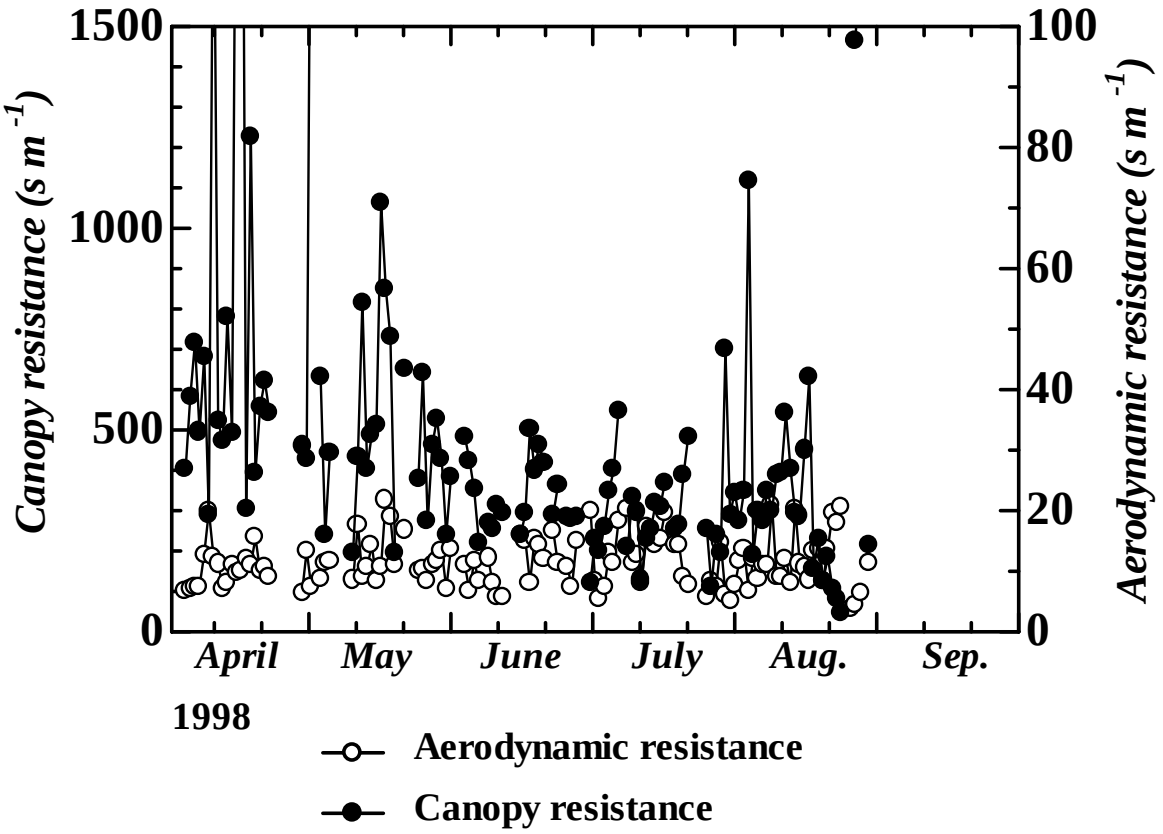
1500
1000
500
0
100
80
60
40
20
0
Canopy resistance (s m-1)
Aerodynamic resistance (s m-1)
April
May
June
July
Aug.
Sep.
1998
Aerodynamic resistance
Canopy resistance

Figure 8

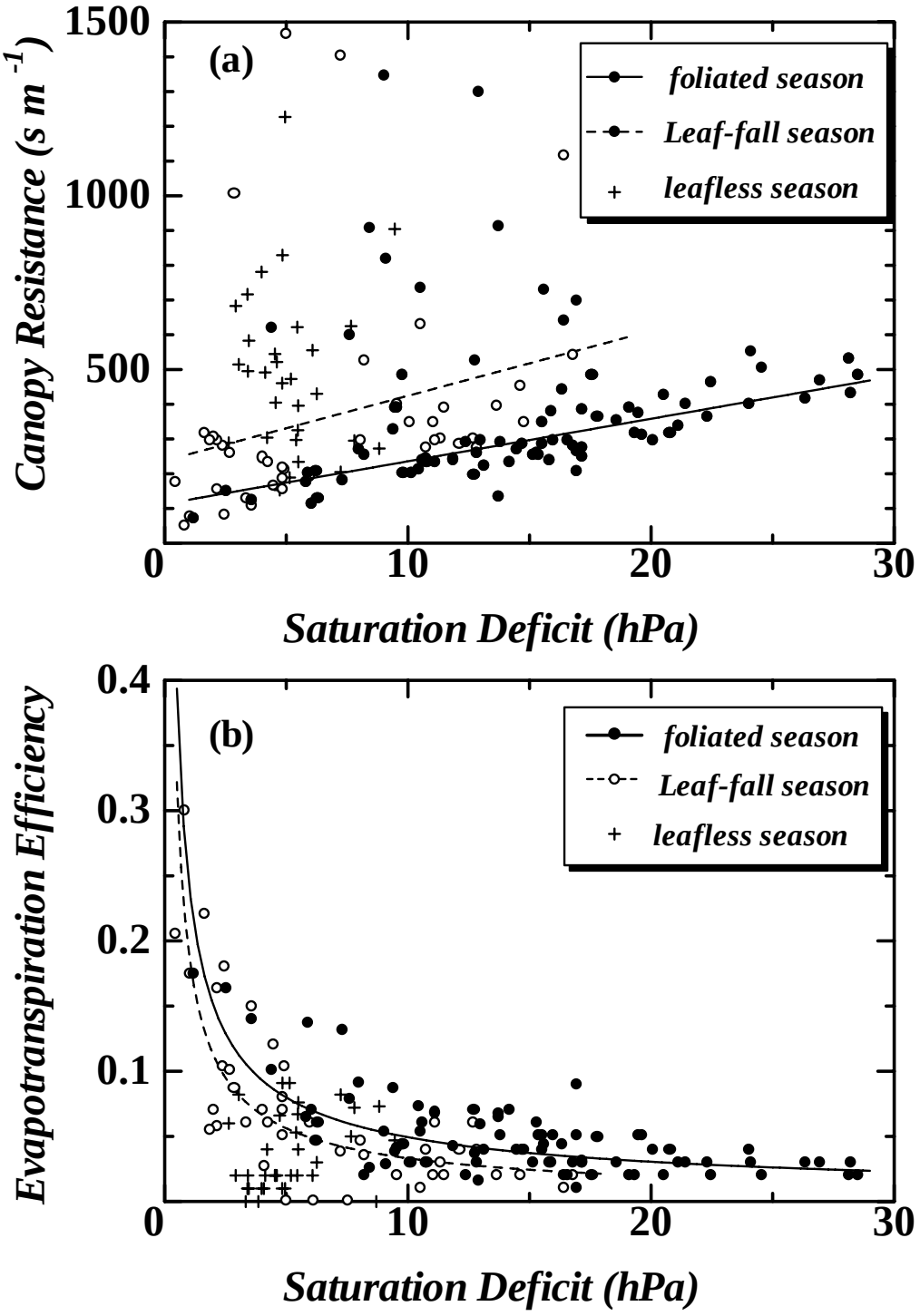
(a)
foliated season
Leaf-fall season
leafless season
Canopy Resistance (s m -1)
1500
1000
500
0
10
20
30
Saturation Deficit (hPa)
(b)
foliated season
Leaf-fall season
leafless season
Evapotranspiration Efficiency
0.4
0.3
0.2
0.1
0
10
20
30
Saturation Deficit (hPa)

Figure 9

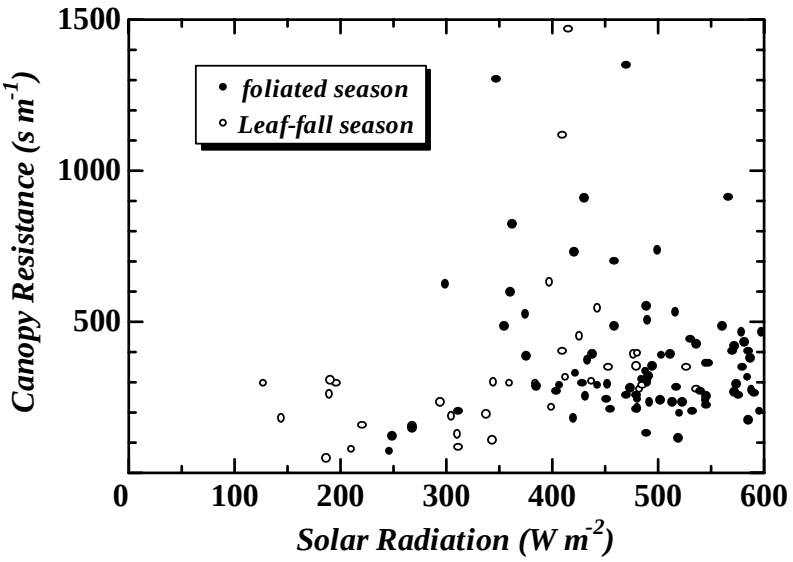
1500
1000
500
0
100
200
300
400
500
600
Canopy Resistance (s m-1)
Solar Radiation (W m-2)
foliated season
Leaf-fall season

Figure 10

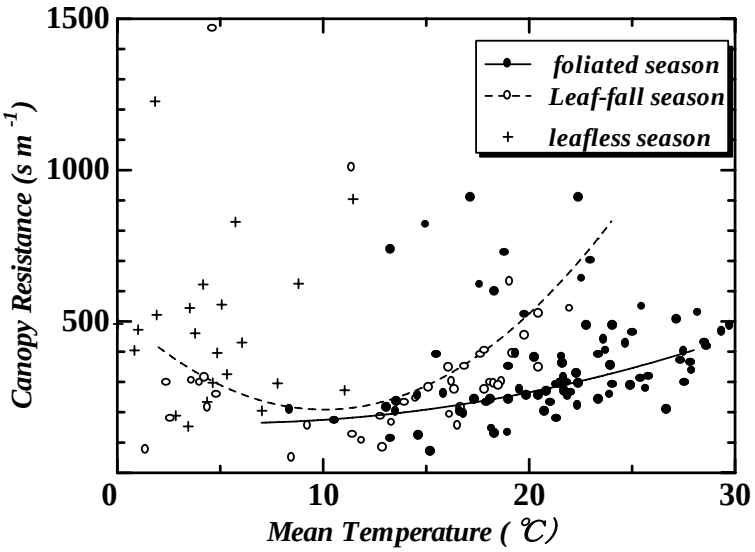
1500
1000
500
0
10
20
30
Canopy Resistance (s m -1)
Mean Temperature (℃)
foliated season
Leaf-fall season
leafless season

Figure 11

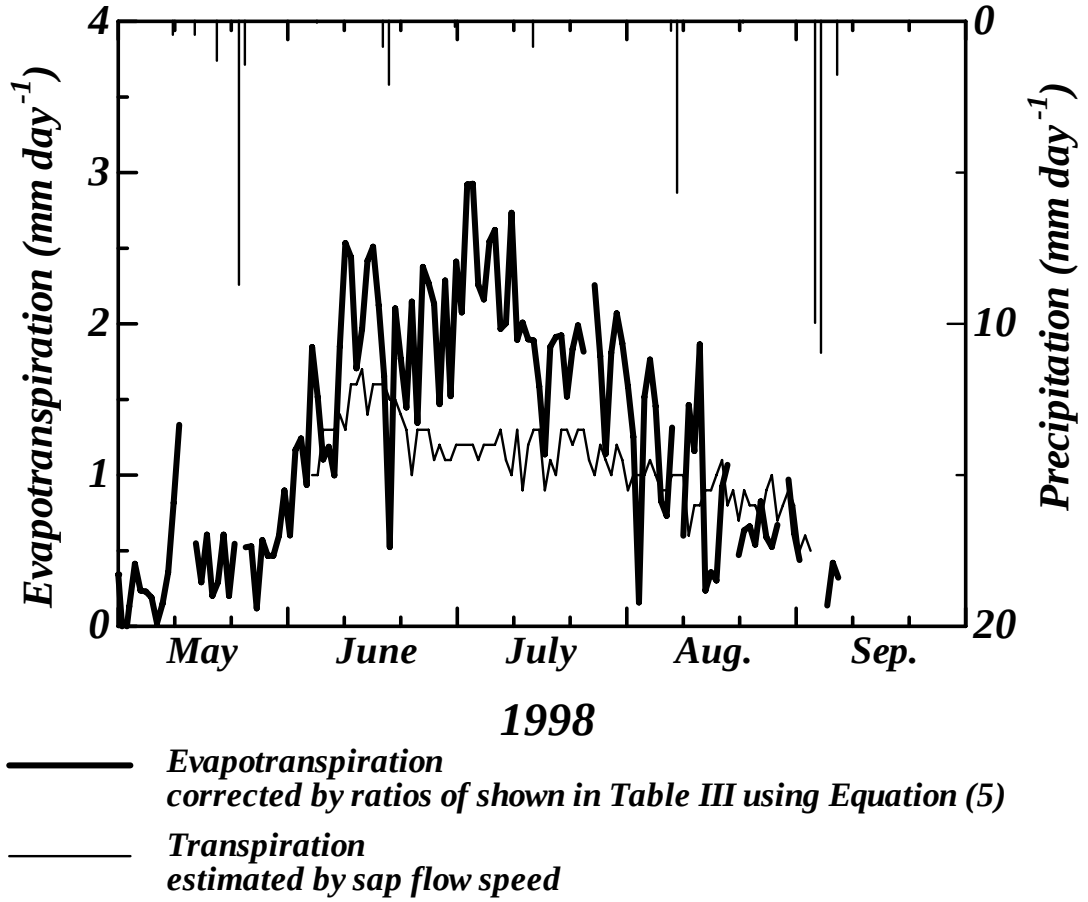
Evapotranspiration (mm day-1)
Precipitation (mm day-1)
4
3
2
1
0
0
10
20
May
June
July
Aug.
Sep.
1998
Evapotranspiration
corrected by ratios of shown in Table III using Equation (5)
Transpiration
estimated by sap flow speed

Figure 12

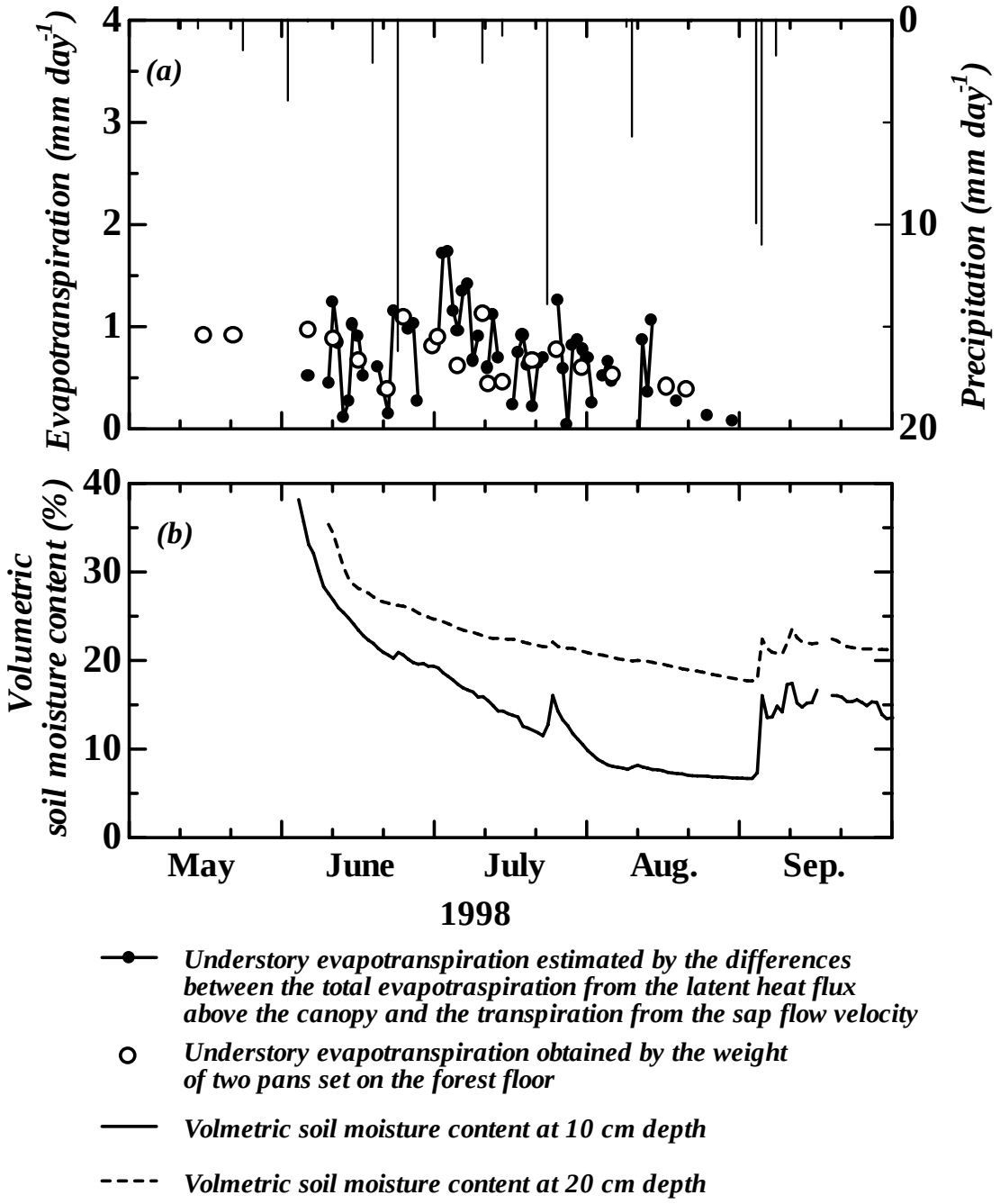
(a)
Evapotranspiration (mm day-1)
Precipitation (mm day-1)
4
3
2
1
0
0
10
20
(b)
Volumetric soil moisture content (%)
40
30
20
10
0
May
June
July
Aug.
Sep.
1998
Understory evapotranspiration estimated by the differences between the total evapotraspiration from the latent heat flux above the canopy and the transpiration from the sap flow velocity
Understory evapotranspiration obtained by the weight of two pans set on the forest floor
Volmetric soil moisture content at 10 cm depth
Volmetric soil moisture content at 20 cm depth